Science of the Total Environment 790 (2021) 148220

Contents lists available at ScienceDirect

Science of the Total Environment

journal homepage: www.elsevier.com/locate/scitotenv

Emissions and light absorption of carbonaceous aerosols from on-road vehicles in an urban tunnel in south China

Runqi Zhang [a,b,d], Sheng Li [a,b,d], Xuewei Fu [a,b,d], Chenglei Pei [d,e], Zuzhao Huang [f], Yujun Wang [e], Yanning Chen [e], Jianhong Yan [g], Jun Wang [a,b,d], Qingqing Yu [a,b], Shilu Luo [a,b,d], Ming Zhu [a,b,d], Zhenfeng Wu [a,b,d], Hua Fang [a,b,d], Shaoxuan Xiao [a,b,d], Xiaoqing Huang [a,b,d], Jianqiang Zeng [a,b,d], Huina Zhang [a,b,d], Wei Song [a,b], Yanli Zhang [a,b,c], Xinhui Bi [a,b], Xinming Wang [a,b,c,d,*]

[a] *State Key Laboratory of Organic Geochemistry and Guangdong Key Laboratory of Environmental Protection and Resources Utilization, Guangzhou Institute of Geochemistry, Chinese Academy of Sciences, Guangzhou 510640, China*
[b] *CAS Center for Excellence in Deep Earth Science, Guangzhou 510640, China*
[c] *Center for Excellence in Regional Atmospheric Environment, Institute of Urban Environment, Chinese Academy of Sciences, Xiamen 361021, China*
[d] *University of Chinese Academy of Sciences, Beijing 100049, China*
[e] *Guangzhou Environmental Monitoring Center, Guangzhou 510030, China*
[f] *Guangzhou Environmental Technology Center, Guangzhou 510180, China*
[g] *Guangzhou Tunnel Development Company, Guangzhou 510133, China*

HIGHLIGHTS

- Carbonaceous aerosols from on-road vehicle fleet were tested in an urban tunnel.
- An average OC/EC ratio of 1.8 ± 1.0 was obtained for the on-road vehicle emission.
- Fleet average EFs of OC and EC were 8.5 ± 6.6 and 4.9 ± 2.6 mg km^{-1}, respectively.
- Regression-derived average TC-EF of 319.8 mg km^{-1} for DVs and 2.1 mg km^{-1} for GVs.
- Brown carbon contributed 19.1% light absorption by carbonaceous aerosols at 405 nm.

GRAPHICAL ABSTRACT

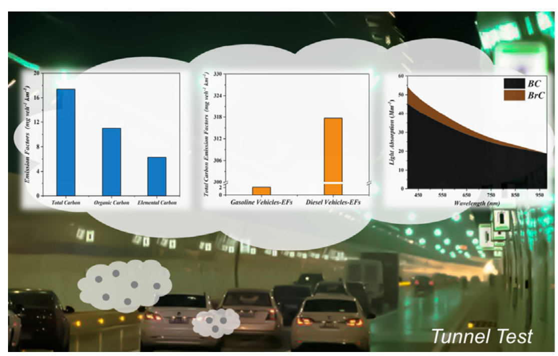

ARTICLE INFO

Article history:
Received 21 March 2021
Received in revised form 11 May 2021
Accepted 29 May 2021
Available online 2 June 2021

Editor: Jianmin Chen

Keywords:
Carbonaceous aerosol

ABSTRACT

With changing numbers, compositions, emission standards and fuel quality of on-road vehicles, it is imperative to accordingly characterize and update vehicular emissions of carbonaceous aerosols for better understanding their health and climatic effects. In this study, a 7-day field campaign was conducted in 2019 in a busy urban tunnel (>30,000 vehicles day^{-1}) in south China with filter-based aerosol samples collected every 2 h at both the inlet and the outlet for measuring carbonaceous aerosols and their light absorbing properties. Observed fleet average emission factor (EF) of total carbon (TC) was 13.4 ± 8.3 mg veh^{-1} km^{-1}, and 17.4 ± 11.3 mg veh^{-1} km^{-1} if electric and LPG-driven vehicles were excluded; and fleet average EF of organic carbon (OC) and elemental carbon (EC) was 8.5 ± 6.6 and 4.9 ± 2.6 mg veh^{-1} km^{-1} (11.0 ± 8.8 and 6.3 ± 3.6 mg veh^{-1} km^{-1} if excluding electric and LPG vehicles), respectively. Regression analysis revealed an average TC-EF of 319.8 mg veh^{-1} km^{-1} for diesel vehicles and 2.1 mg veh^{-1} km^{-1} for gasoline vehicles, and although diesel vehicles only shared ~4% in the fleet

* Corresponding author at: State Key Laboratory of Organic Geochemistry and Guangdong Key Laboratory of Environmental Protection and Resources Utilization, Guangzhou Institute of Geochemistry, Chinese Academy of Sciences, Guangzhou 510640, China.
E-mail address: wangxm@gig.ac.cn (X. Wang).

https://doi.org/10.1016/j.scitotenv.2021.148220

On-road vehicles
Emission factors
Light absorption
Tunnel test
Black carbon
Brown carbon

compositions, they still dominate on-road vehicular carbonaceous aerosol emissions due to their over 150 times higher average TC-EF than gasoline vehicles. Filter-based light absorption measurement demonstrated that on average brown carbon (BrC) could account for 19.1% of the total carbonaceous light absorption at 405 nm, and the average mass absorption efficiency of EC at 635 nm and that of OC at 405 nm were 5.2 $m^2\ g^{-1}$ C and 1.0 $m^2\ g^{-1}$ C, respectively.

1. Introduction

Carbonaceous aerosols have significant effects on air quality (Cao et al., 2012; Che et al., 2007; Wu et al., 2007), human health (Maji et al., 2018; Shang et al., 2013; Tie et al., 2009), and climate change (Akimoto, 2003; Ramanathan et al., 2001). Carbonaceous aerosols are very complex mixtures, consisting of organic carbon (OC) and a refractory carbon component, which refers to the elemental carbon (EC, when quantified by thermally optical method) or black carbon (BC, it is called equivalent black carbon (eBC) when quantified by optical method) (Chow and Watson, 2002; Petzold et al., 2013; Contini et al., 2018). As an important short-lived climatic pollutant, BC poses direct warming effects only less than CO_2 (Bond et al., 2013), and thus emission control of BC is of increasing concern for co-benefits in reducing both health risks and global warming potentials. Organic carbon (OC), as the major component of carbonaceous aerosols, is considered as a pure scattering aerosol in early studies and therefore may have a cooling effect on the climate (Bond et al., 2013; Bond et al., 2004; Mordukhovich et al., 2009; Ramanathan et al., 2007). However, recent studies have revealed that light-absorbing compounds, termed brown carbon (BrC), are present in OC, introducing large uncertainties to current climate models (Feng et al., 2013; Jo et al., 2016). BrC may contribute about 10–30% of total light absorption of airborne fine particles at 365 nm and 405 nm (Clarke et al., 2007; Favez et al., 2009; Sun et al., 2007; Yang et al., 2009). BrC from biomass burning, in particular, could even contribute more than 65% of light absorption at 370 nm (Favez et al., 2009). As China has become the largest emitter of carbonaceous aerosols (Bond et al., 2007; Cofala et al., 2007) with approximately one-fourth of global carbonaceous aerosol emissions (Bond et al., 2007; Cofala et al., 2007), controlling short-lived climate pollutants like carbonaceous aerosols in China has the potential to yield more immediate climate benefits than controlling long-lived climate pollutants, such as carbon dioxide (CO_2) (Schmale et al., 2014; Shindell et al., 2012).

Vehicle emissions are an important source of carbonaceous aerosols, especially in urban areas. Bond et al. (2004) pointed out that globally vehicle exhausts could contribute 11.5% of the total BC emissions. As estimated by Wang et al. (2012), vehicle emissions could account for 9.4% of China's BC emissions in 2007, of which diesel and gasoline vehicles shared 8.0% and 1.4%, respectively. In urban areas, vehicular emission could contribute up to 50% of total carbonaceous aerosols (Almeida et al., 2005; Maykut et al., 2003; Yu et al., 2013). Since vehicular emissions are highly dynamic with the changing engine technology, after-treatment performance, and tightening emission standards, it is imperative to accordingly characterize carbonaceous aerosol emissions from on-road vehicles and timely update the emission estimates. As a matter of fact, emissions of air pollutants from vehicles would decrease significantly with stricter emission standards (Zhao et al., 2018).

There are a variety of approaches to characterizing vehicle emissions, such as chassis and engine dynamometer testing (Artelt et al., 1999), roadside measurements (Bishop and Stedman, 1996), portable emissions measurements (Yao et al., 2015), and tunnel tests (Zhang et al., 2015). Among these approaches, tunnel tests could obtain emissions for on-road vehicle fleets under real-world driving conditions (Chirico et al., 2011), and there have been some studies in China to measure emission factor (EF) of carbonaceous aerosols based on tunnel tests, mainly in the Pearl River Delta region, the world's largest megacity in south China. Studies in the Shing Mun Tunnel in Hong Kong revealed that fleet-average EF of total carbon (TC; the sum of OC + EC) had decreased greatly from 101.5 mg veh^{-1} km^{-1} in 2003 (Cheng et al., 2011) to 22.2 mg veh^{-1} km^{-1} in 2015 (Niu et al., 2020), probably due to the implementation of Euro V emission standard in 2007. However, Chiang and Huang (2009) observed that a fleet-average TC-EF of 19.8 mg veh^{-1} km^{-1} based on tests in the Chung-Liao Tunnel in Hong Kong in 2019, and the TC was OC-dominating instead of EC-dominating as observed in the Shing Mun Tunnel. The differences in emissions of carbonaceous aerosols from the two tunnel tests in Hong Kong might result from their different fleet compositions, which is an important factor influencing carbonaceous aerosol emissions as demonstrated in previous studies (Alander et al., 2004; Robert et al., 2007; Yang et al., 2019). In the Zhujiang Tunnel, a busy urban tunnel in Guangzhou and the same tunnel where this study was conducted, emission factors and compositions of carbonaceous aerosols were measured in 2004, 2013, and 2014, respectively (He et al., 2008; Dai et al., 2015; Zhang et al., 2015). Liu et al. (2012) reported EF of carbonaceous aerosols based on the tests in 2010 in an urban tunnel in Shenzhen, a big city neighboring Hong Kong. In north China, Cui et al. (2016) compared emissions and composition profiles of $PM_{2.5}$ in both an urban tunnel and a suburban tunnel in 2014 in Yantai, and pointed out that vehicle types and driving conditions could affect carbonaceous aerosol compositions and emissions. For the light absorption of carbonaceous aerosols from on-road vehicles in China, only one study is available with roadway tunnel experiments (Yuan et al., 2016).

In recent years, the number of vehicles in China rose rapidly from 170 million in 2014 to 348 million in 2019 (http://www.mee.gov.cn/hjzl/sthjzk/ydyhjgl/). Meanwhile, vehicle emission standards have been updated from China IV in 2010 to China V in 2015 and to China VI in 2020. Therefore, it is necessary to update vehicular EF for carbonaceous aerosols with the rapid changes. In essence, measurements in the Zhujiang Tunnel have revealed great changes in on-road vehicular emissions during 2004–2014 (He et al., 2008; Zhang et al., 2015, 2018). Here we renewed our tests in the Zhujiang Tunnel in 2019, and this study aims to: (1) update EF of carbonaceous aerosols and assess the effectiveness of vehicle emission control in reducing carbonaceous aerosol emissions by comparing with previous studies in the same tunnel; (2) investigate the light-absorption properties of vehicular carbonaceous aerosols; and (3) quantitatively estimate contributions to light absorption by BC and BrC emitted by on-road vehicles under real-world driving conditions.

2. Experimental

2.1. Tunnel sampling

The field campaign was conducted in the Zhujiang Tunnel (23.13°N, 113.25°E) in urban Guangzhou during October 13–19, 2019. The tunnel is 1238 m in length, consisting of a 721 m flat underwater section and two 517 m open slope sections. Sampling sites were located 50 m away from the entrance and outlet of the flat underwater section, respectively (Fig. 1). The detailed descriptions of the tunnel were given elsewhere (Zhang et al., 2015). The ventilation systems in the tunnel were all closed during the sampling period to ensure that the accumulation of particulate matter inside the tunnel was solely attributed to vehicle emissions.

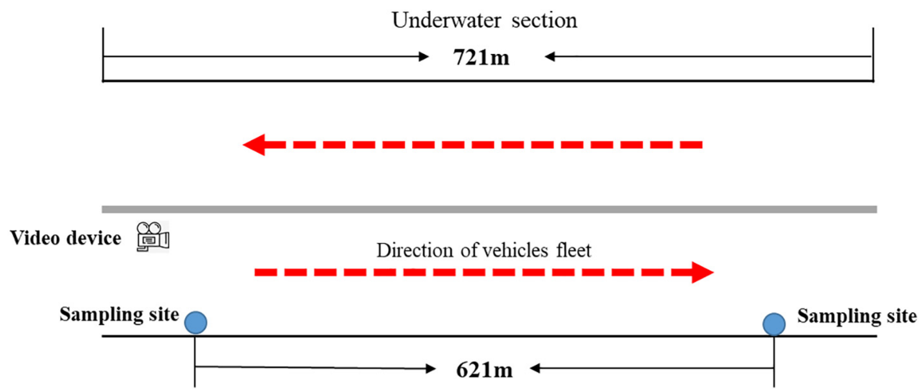

Fig. 1. Schematic diagram of sampling sites in the Zhujiang Tunnel.

Filter-based $PM_{2.5}$ samples were collected concurrently at both the inlet and the outlet stations by high-volume samplers (TE-6070, Tisch Environmental Inc., USA) at a constant flow rate of 1.1 ± 0.04 $m^3 \cdot min^{-1}$ during each 2-h intervals, namely 0:00–2:00, 02:00–04:00, 04:00–06:00, 06:00–08:00, 08:00–10:00, 10:00–12:00, 12:00–14:00, 14:00–16:00, 16:00–18:00, 18:00–20:00, 20:00–22:00 and 22:00–24:00. Before sampling, the quartz filters (8 × 10 in., Whatman, UK) were prebaked at 450 °C for 4 h to eliminate any interference from the filters. All collected samples were stored in a refrigerator at −20 °C before chemical analysis. The blank samples were collected by loading the filter onto the sampler without starting the sampler.

The meteorological parameters, such as wind speed and temperature, were synchronously measured at the entrance and the exit sampling locations by a 3-D Sonic Anemometer. The accuracy of the 3-D Sonic Anemometer in measuring wind direction, horizontal wind, and ambient temperature is ±0.7°, 1 m s^{-1} and ± 0.5 °C, respectively. More detailed descriptions about the 3-D Sonic Anemometer can be found in our previous study (Zhang et al., 2015). A video camera was placed at the entrance during the sampling periods. The videotapes were used to count vehicle number and to categorize the vehicles into four categories by fuel-types, namely, diesel vehicles (DVs) (including heavy-duty trucks, medium-duty trucks, large passenger cars, and medium passenger cars), gasoline vehicles (GVs) (including sedan cars with blue license plates, light-duty trucks, light passenger cars, and motorcycles), electric vehicles (EVs) (including sedan cars with green license plates, taxis, buses with green license plates), and liquefied petroleum gas vehicles (LPGVs) (including taxies with blue license plates) (He et al., 2005).

2.2. Chemical analysis

Organic carbon and elemental carbon in $PM_{2.5}$ were analyzed by a DRI Model 2015 multi-wavelength thermal/optical carbon analyzer (Desert Research Institute, Nevada, USA). A circular punch (0.5024 cm^2) of the filters was taken into the quartz groove and analyzed by an IMPROVE_A heating procedure. This heating procedure included four OC fractions (OC1, OC2, OC3, and OC4 with cutting temperature of 140, 280, 480, and 580 °C, respectively, in a helium atmosphere) and three EC fractions (EC1, EC2, and EC3 with cutting temperature of 580, 740, and 840 °C, respectively, in an oxygen/helium atmosphere of 2/98 volume ratio). Meanwhile, this analyzer, which was equipped with seven diode lasers (405, 455, 532, 635, 780, 808, and 980 nm), can also be used to determine the spectral reflectance and transmittance of filter samples. During the analysis of samples, the stability and reliability of the instrument are tested daily with standard potassium phthalate (Li et al., 2018).

2.3. Calculation of emission factors

Average emission factors (EF) for vehicles traveling through the tunnel during a time interval were calculated the same way as in previous studies (Zhang et al., 2015)

$$EF_i = \frac{(C_{i,out} - C_{i,in}) \times V_{air} \times T \times A}{N \times L} \tag{1}$$

where EF_i (mg veh^{-1} km^{-1}) is the emission factor of i species; $C_{i,out}$ and $C_{i,in}$ (mg m^{-3}) are the concentration of i species at the tunnel exit and entrance, respectively; V_{air} (m s^{-1}) is the air velocity parallel to the tunnel sensed by the 3-D sonic anemometer; A is the tunnel cross-section area, which is 52.8 m^2 in this study; N is the total traffic number traveling through the tunnel during the time interval T (s) ($T = 7200$ s in this study), and L is the length of the tunnel between the two monitoring locations, which is 0.621 km in this study.

2.4. Calculation of light absorption coefficient

The light absorption coefficient (b_{abs}) for particles was estimated by Eq. (2) as described in detail in previous studies (Chen et al., 2015; Li et al., 2018):

$$b_{abs} = \left[A_\lambda \times ln\left(\frac{FT_{\lambda,f}}{FT_{\lambda,i}}\right)\right]^2 + B_\lambda \times ln\left(\frac{FT_{\lambda,f}}{FT_{\lambda,i}}\right) \times \frac{A}{V} \tag{2}$$

where A_λ and B_λ are coefficients describing wavelength-specific multiple-scattering and loading effects, respectively, and the values of A_λ and B_λ were reported by Chen et al. (2015); $FT_{\lambda,i}$ and $FT_{\lambda,f}$ are the filter transmittance measured before and after thermal analysis, respectively, and here $FT_{\lambda,f}$ approximates the transmittance of a blank filter; A is the filter area, and V is the sampling volume.

Since BC and BrC are the light-absorbing materials in the aerosol samples, a simplified two-component model was used to differentiate their relative contributions to light absorption (Chen et al., 2015; Li et al., 2018):

$$b_{abs} = \left(K_{BC} \times \lambda^{-AAE_{BC}} + K_{BrC} \times \lambda^{-AAE_{BrC}}\right) \times \frac{A}{V} \tag{3}$$

where K_{BC} and K_{BrC} are the fitting coefficients for BC and BrC, respectively; AAE_{BC} and AAE_{BrC} are the absorption Angstrom exponent values of BC and BrC, respectively. Previous studies have shown that when particulate matter is mainly emitted from the high-temperature combustion process of motor vehicles, its corresponding AAE value of BC is close to 1 (Bergstrom et al., 2002; Bond and Bergstrom, 2006; Drozd and McNeill, 2014; Yuan et al., 2016).

Therefore, in this study, we assume that AAE_{BC} value is 1.0. And, the corresponding mass absorption efficiency (MAE, $m^2\ g^{-1}$ C) could be calculated in the following formula:

$$MAE = \frac{\Delta b_{abs}}{\Delta carbonaceous\ aerosols} \tag{4}$$

where Δcarbonaceous aerosols are the incremental carbonaceous aerosols concentrations (μg m^{-3}).

3. Results and discussion

3.1. Traffic fleets and carbonaceous aerosol concentrations inside the tunnel

During the sampling campaign, the traffic volume in the tunnel varied from 34,141 to 37,721 vehicles day^{-1}, and its daily maximums occurred between 16:00–18:00 with an average of 4170 vehicles h^{-1}. The traffic volume was higher during the daytime (8:00–20:00) with an average of 3765 vehicles h^{-1}our compared to that during the nighttime with an average of 2211 vehicles h^{-1}. The temporal variation in GVs, DVs, EVs, and LPGVs during the sampling period were shown in Fig. 2. On average, GVs, EVs, LPGVs, and DVs accounted for 75.1%, 13.3%, 7.8%, and 3.8%, respectively. Unlike the fleet compositions observed in the same tunnel in 2014 (Zhang et al., 2015), the number of EVs increased rapidly in recent five years, and EVs replaced DVs to become the second-largest in the vehicle fleets (Fig. 7).

The average incremental concentrations from inlet to outlet for OC and EC, termed ΔOC and ΔEC, were 9.8 ± 6.4 μg m^{-3} and 6.0 ± 3.2 μg m^{-3}; and they were 67.0% and 68.6% lower than those observed in the same tunnel in 2014 (Zhang et al., 2015), respectively. The ΔOC/ΔEC ratios ranged from 0.2 to 5.7 with an average of 1.8 ± 1.0. The dominance of GVs in the fleet in this study makes the average OC/EC ratio much higher than those in tunnels with a larger portion of DVs traveling through, such as 0.76 in Sepulveda tunnel, USA (Gillies et al., 2001), 0.21 in Bulk-Ak tunnel, Korea (Ma et al., 2004), 0.20 in Kaisermuhlen tunnel, Austria (Handler et al., 2008), 0.53 in an urban tunnel, France (El Haddad et al., 2009), and 0.29–0.37 in Marques de Pombal tunnel, Portugal (Pio et al., 2011). This difference in the OC/EC ratios is also consistent with dynamometer test results, which demonstrated that the higher OC/EC ratios (>1) were associated with gasoline vehicle emissions while lower values (0.2–0.9) were associated with diesel vehicle emissions (Alander et al., 2004; Robert et al., 2007; Yang et al., 2019).

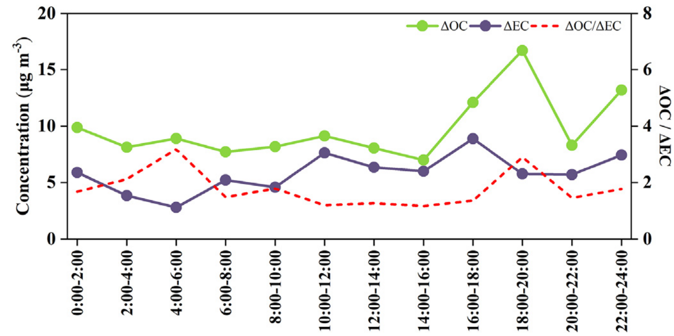

Fig. 3. Average diurnal variations of ΔOC and ΔEC concentrations during the sampling period.

ΔOC and ΔEC showed great diurnal variations, but not in a consistent way (Fig. 3). It was found that the variation in ΔOC and ΔEC concentrations was associated with the traffic fleet compositions (the proportions of GVs and DVs) (Alander et al., 2004; Robert et al., 2007; Yang et al., 2019). For example, during 4:00–6:00, ΔOC had a small peak while ΔEC dropped to the lowest, largely due to increases in the proportion of GVs at this time intervals. At the beginning of the morning rush hour (4:00–6:00), the number of GVs had risen sharply, while the number of DVs had remained stable or even declined. Similarly, during 18:00–20:00, ΔEC decreased significantly while ΔOC increased to reach a peak because DVs were prohibited from entering the urban areas, leading to a sharp drop in numbers of DVs between 17:00 and 20:00.

3.2. Emission factors of carbonaceous aerosols

The fleet average EF for TC was 13.4 ± 8.3 mg $veh^{-1}\ km^{-1}$, in which EF for OC and EC was 8.5 ± 6.6 and 4.9 ± 2.6 mg $veh^{-1}\ km^{-1}$, respectively. As EVs have no emission of carbonaceous aerosols and emissions of carbonaceous from LPGVs can be negligible (Zhai et al., 2007; Ristovski et al., 2005; Stewart et al., 2021; Wang et al., 2013; Wang et al., 2004), if LPGVs and EVs are excluded, the average TC-EF for GVs and DVs should be 17.4 ± 11.3 mg $veh^{-1}\ km^{-1}$, and the EF for OC and EC was 11.0 ± 8.8 and 6.3 ± 3.6 mg $veh^{-1}\ km^{-1}$, respectively.

To explore the trend of carbonaceous aerosol emission from on-road vehicles with the increasingly tightened vehicle emission standards and

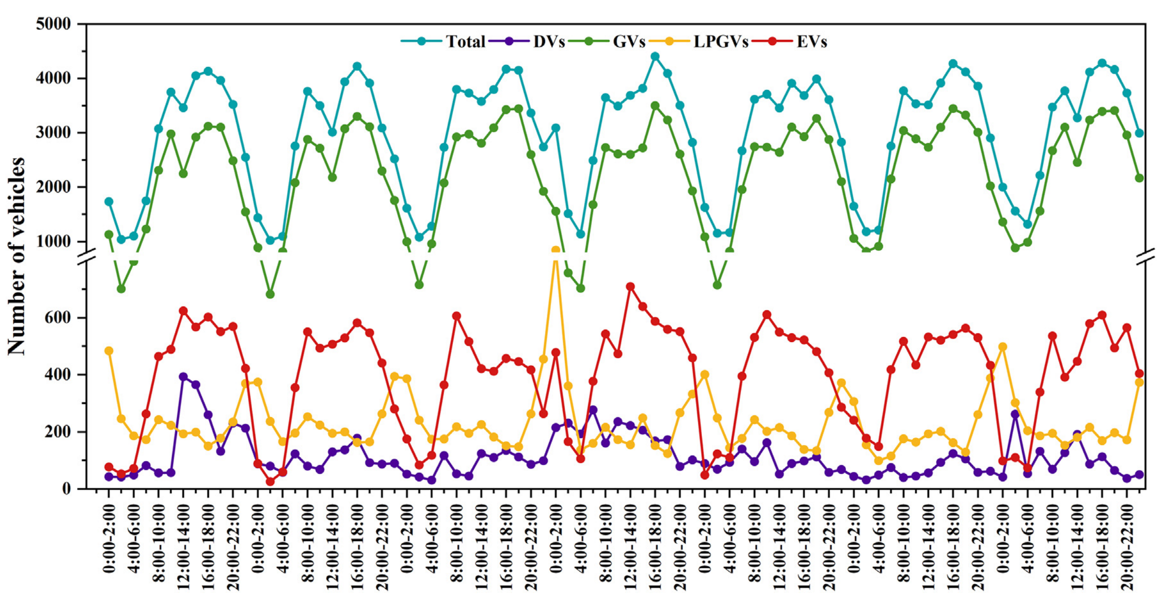

Fig. 2. Diurnal variations of different fuel-type vehicles during the sampling period.

Table 1
EFs of carbonaceous aerosols from this study in comparison with those from previous tunnel studies.

Study area-test year	Emission factors (mg veh^{-1} km^{-1})			References
	OC	EC	TC	
Monterrey Tunnel, USA-2009	12.6	5.7	18.3	(Mancilla and Mendoza, 2012)
Kiborn Tunnel, USA-2000	6.4	6.9	13.3	(Lough et al., 2005)
Howell Tunnel, USA-2000	12.9	6.6	19.5	
Kaisernuhlen Tunnel, Austria-2005	5.4	17.8	23.2	(Handler et al., 2008)
Sepulveda Tunnel, USA-1996	19.3	25.5	44.8	(Gillies et al., 2001)
Osmangazi Tunnel, Turkey-2018	40.3	33.7	74.0	(Gaga et al., 2018)
Shing Mun Tunnel, Hong Kong-2003	35.7	65.8	101.5	(Cheng et al., 2011)
Shing Mun Tunnel, Hong Kong-2015	6.6	15.6	22.2	(Niu et al., 2020)
Chung-Liao Tunnel, Taiwan-2009	15.1	4.7	19.8	(Chiang and Huang, 2009)
Shenzhen Tunnel, Shenzhen-2010	9.7	20.2	29.9	(Liu et al., 2012)
WZS Tunnel, Yantai-2014	19.4	22.5	41.9	(Cui et al., 2016)
KXL Tunnel, Yantai-2014	3.9	2.3	6.2	
Zhujiang Tunnel, Guangzhou-2004	24.3	49.6	73.9	(He et al., 2008)
Zhujiang Tunnel, Guangzhou-2013	16.7	16.4	33.1	(Dai et al., 2015)
Zhujiang Tunnel, Guangzhou-2014	19.3	13.3	32.6	(Zhang et al., 2015)
Zhujiang Tunnel, Guangzhou-2019	8.5	4.9	13.4	This study

changing fleet compositions, we compared the results from this study with those from previous studies, as showed in Table 1. Compared with that from other tunnel studies over the world, the average TC-EF of the entire fleet (13.4 mg veh^{-1} km^{-1}) from this study was similar to that of 13.3 mg veh^{-1} km^{-1} observed in 2000 in Kilborn tunnel in Milwaukee, America, and only higher than that of 6.2 mg veh^{-1} km^{-1} observed in 2014 at the suburban KXL tunnel in Yantai, China (Table 1). The fleet OC-EF of 8.5 mg veh^{-1} km^{-1} was at a relatively low level, but still higher than that of 6.4 mg veh^{-1} km^{-1} observed in 2000 at the Kilborn tunnel, 5.4 mg veh^{-1} km^{-1} in 2005 at the Kaisernuhlen tunnel, and 6.6 mg veh^{-1} km^{-1} in 2015 at the Shing Mun tunnel; Similarly, the fleet EC-EF of 4.9 mg veh^{-1} km^{-1} was much lower when compared to that ranging 5.7–65.8 mg veh^{-1} km^{-1} reported in other tunnel studies (Cui et al., 2016; Gaga et al., 2018; Gillies et al., 2001; Handler et al., 2008; Liu et al., 2012; Lough et al., 2005; Mancilla and Mendoza, 2012; Niu et al., 2020), except that an EC-EF as low as 4.7 mg veh^{-1} km^{-1} was observed in the Chung-Liao tunnel in Taiwan (Chiang and Huang, 2009). Compared with other studies, the low EC-EF in this study may be resulted from a lower proportion of DVs (Alander et al., 2004; Robert et al., 2007; Yang et al., 2019) and tighter emissions standards (Zhang et al., 2015).

Compared with the previous studies in the same tunnel (He et al., 2008; Zhang et al., 2015), measured average TC-EF decreased by 59.0% from 2014 to 2019, in which the EF of OC and EC decreased by 56.0% and 63.5%, respectively. The significant reduction in carbonaceous aerosol emissions was mainly due to changes in fuels and emission standards (He et al., 2008; Shen et al., 2014; Zhang et al., 2015; Niu et al., 2020). In the city of Guangzhou, since 2004 public transportation vehicles such as buses and taxis had been converted from diesel- and gasoline-driven to LPG-driven and electric-driven (He et al., 2008; Zhang et al., 2015). By 2018, all buses had been switched to electric-driven ones, all taxis had been switched to electric-driven or LPG-driven ones, and the number of electric-driven private cars had also increased rapidly. On the other hand, upgrading motor vehicle emissions standards was also an important factor leading to a significant reduction in vehicle emissions (Shen et al., 2014). Emission standards of particulate matter from vehicles were upgraded from 0.08 to 0.20 g km^{-1} in China II (GB18352.2-2001) to 0.0045 g km^{-1} in China V (or Euro V) (GB 18352.5-2013). By 2018, the proportion of motor vehicles meeting the emission standards of China IV and above reached up to 73.4% (Zhang et al., 2015).

As EVs have no emission of carbonaceous aerosols and emissions of carbonaceous from LPGVs are negligible, we can ascribe emissions of carbonaceous aerosols in the tunnel to diesel and gasoline vehicles, and average EF for diesel and gasoline vehicles can be derived from regression based on the following equation (Zhang et al., 2015):

$$EF_i = \alpha_i \times EF_{diesel} + (1-\alpha_i) \times EF_{gasoline} \quad (5)$$

where EF_i is the fleet average EF excluding EVs and LPGVs during time inter i, α_i is the fraction of DVs during time interval i, EF_{diesel} is the average emission factor for DVs, and $EF_{gasoline}$ is the average emission factor for GVs. Based on the regression analysis, an average TC-EF was derived to be 319.8 ± 65.1 mg veh^{-1} km^{-1} for DVs and 2.1 ± 3.6 mg veh^{-1} km^{-1} for GVs. Based on the regression results, although the proportion of DVs was only ~4% in the fleet, they contributed over 88% of carbonaceous aerosols from on-road vehicles since the average TC-EF for DVs was over 150 times higher than that for GVs.

A comparison of our results with those reported from previous tunnel studies based on the same regression method was shown in Table 2. Compared with other studies, The GV-EF in this study were only higher than that of 1.0 mg veh^{-1} km^{-1} observed in 2014 in Yantai, China (Cui et al., 2016), but significantly lower than that from other tunnel studies (Table 2). In the same tunnel, the GV-EF measured in 2004 by He et al. (2008) was 16.7 times that measured from this study in 2019, largely due to the upgrading of emission standards in the study area. The DV-

Table 2
Comparison of TC-EFs (mg veh^{-1} km^{-1}) for DVs and GVs derived from regression in this study with those in previous studies.

Study area-test year	TC-EFs	Vehicle type
Caldecott Tunnel, San Francisco, USA-1997[a]	3.5	Light-duty vehicle
	428.0	High duty vehicle
Shing Mun Tunnel, Hong Kong, China-2003[b]	11.7	Light-duty vehicle
	198.9	High duty vehicle
Shenzhen Tunnel, Shenzhen, China-2010[c]	8.7	Light-duty vehicle
	124.4	High duty vehicle
Zhujiang Tunnel, Guangzhou, China-2004[d]	35.0	Light-duty vehicle
	217.0	High duty vehicle
WZS Tunnel, Yantai, China-2014[e];	1.0	Gasoline vehicle
KXL Tunnel, Yantai, China-2014[e]	277.0	Diesel vehicle
Zhujiang Tunnel, Guangzhou, China-2019[f]	2.1	Gasoline vehicle
	317.7	Diesel vehicle

[a] (Allen et al., 2001).
[b] (Cheng et al., 2011).
[c] (Liu et al., 2012).
[d] (He et al., 2008).
[e] (Cui et al., 2016).
[f] This study.

EF from this study were significantly higher when compared to those in other tunnels (Cheng et al., 2011; Liu et al., 2012; He et al., 2008; Cui et al., 2016), except that of 428.0 mg veh^{-1} km^{-1} observed at the Caldecott tunnel (Allen et al., 2001). A previous study indicated that TC-EF for DVs increased with the increase of vehicle passenger volume or cargo capacity with the same emission standards (Zhao et al., 2019a). Apart from that a high proportion of DVs were heavy-duty ones (42.4%), most DVs in the fleets were China III and China IV (equivalent to Euro III and IV) ones without after-treatment systems. Therefore, a relatively higher average TC-EF was observed for DVs from this study.

3.3. Light absorption of BC and BrC

Time series of the TC light-absorption (babs-TC) at three wavelengths (405, 455, and 635 nm) are shown in Fig. 4. On average $b_{abs\text{-}TC}$ at 405, 455, and 635 nm were 15.7 ± 6.9 Mm^{-1}, 13.3 ± 5.6 Mm^{-1} and 7.7 ± 3.6 Mm^{-1} at the inlet, and were 66.2 ± 29.8 Mm^{-1}, 58.6 ± 26.3 Mm^{-1} and 38.3 ± 18.1 Mm^{-1} at the outlet, respectively. On average $\Delta b_{abs\text{-}TC}$ at 405, 455 and 635 nm were 52.5 ± 29.0 Mm^{-1}, 47.2 ± 25.2 Mm^{-1} and 31.8 ± 17.4 Mm^{-1}, respectively. The mass absorption efficiency (MAE, m^2 g^{-1} C) of carbonaceous aerosols is an important parameter for the derivation of aerosol particle radiative forcing in climate models. Calculated average MAE_{TC} at 405, 455, and 635 nm were 3.6 ± 2.1, 3.2 ± 1.8, and 2.1 ± 1.3 m^2 g^{-1} C, respectively. These results were similar to $MAE_{405\ nm}$ (3.4 m^2 g^{-1} C in summer; 4.9 m^2 g^{-1} C in autumn) measured by Li et al. (2018) in 2015 using the same approach for filter-based ambient carbonaceous aerosols at an urban site about 4 km away from the Zhujiang Tunnel. The light absorption of TC can be further divided into that of BC and BrC (Chow and Watson, 2002). As shown in Fig. 5, nonlinear regression based on Eq. (3) revealed that light absorption by BC ($b_{abs\text{-}BC}$) at 405, 455 and 635 nm were 45.5 ± 28.2, 41.4 ± 25.7, and 29.0 ± 18.0 Mm^{-1}, accounting for 80.9 ± 12.3%, 81.6 ± 11.7%, and 86.5 ± 9.1% of $b_{abs\text{-}TC}$, while BrC accounted for 19.1 ± 12.3%, 18.4 ± 11.7%, and 13.5 ± 9.1%, respectively (Fig. 6).

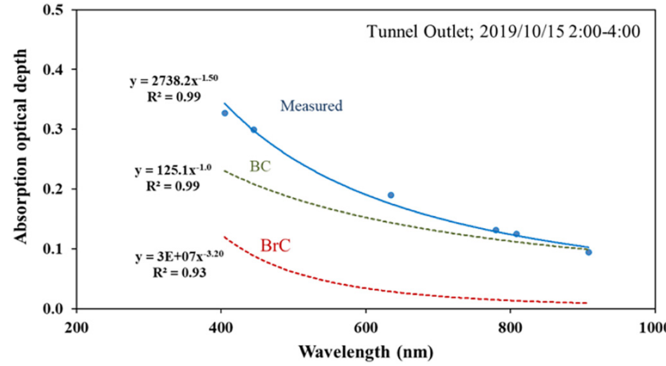

Fig. 5. An example showing the decomposition of contributions to the measured absorption optical depth by BC and BrC for a $PM_{2.5}$ filter sample collected at the outlet.

According to a previous study (Hecobian et al., 2010), the wavelength of 405 nm and 635 nm was selected to characterize the MAE of OC and EC, respectively. The fleet average MAE_{635nm} of EC from this study was 5.2 ± 3.1 m^2 g^{-1} C. In previous studies, Yan et al. (2019) found that MAE_{632nm} for EC from vehicle emissions were significantly higher than those from other sources, such as 11.2 m^2 g^{-1} C for EC from gasoline vehicle emissions, 7.0 m^2 g^{-1} C for EC from ship emissions, 6.6 m^2 g^{-1} C for EC from diesel exhaust, 5.5 m^2 g^{-1} C for EC from coal combustion in quartz tube furnace, 4.9 m^2 g^{-1} C for EC from coal combustion in household coal stoves, 4.5 m^2 g^{-1} C for EC from industry emissions, and 0.5 m^2 g^{-1} C for EC from power plant emissions. Schwarz et al. (2008) and Cheng et al. (2011) also indicated that the MAE_{EC} from vehicle emissions were significantly higher (~8 m^2 g^{-1} C). In this study, the measured $MAE_{635\ nm}$ of EC is lower than those

Fig. 4. Diurnal variations of $PM_{2.5}$ light absorption at the tunnel outlet and the inlet.

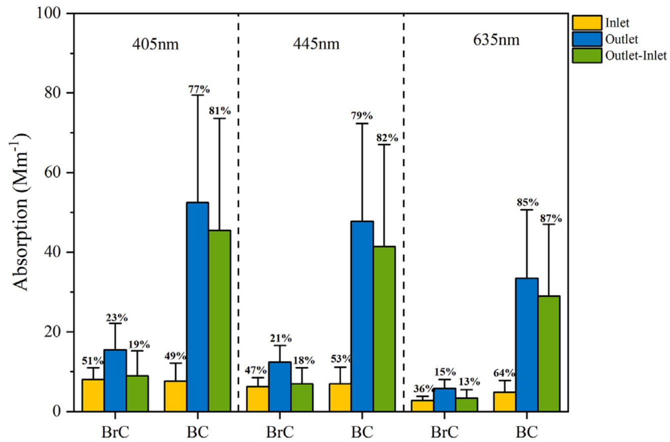

Fig. 6. The average light absorption of BC and BrC at 405, 445 and 635 nm. The percentages over the bars are the contribution percentages in the total light absorption.

Table 3
Comparison of MAE_{OC} from our tunnel tests with those by solvent extraction method.

Source types	MAE_{OC} ($m^2\ g^{-1}$ C)	Reference
	WSOC (365 nm)	
Biomass burning	1.6 ± 0.6	(Tang et al., 2020)
Anthracite combustion	1.3 ± 0.3	
Bituminous coal combustion	2.0 ± 0.75	
Vehicle emission	0.71 ± 0.30	
Coal combustion	0.9–1.0 for anthracite 0.3–0.7 for bituminous coal	(Li et al., 2019)
Rice straw burning	1.37 ± 0.23	(Park and Yu, 2016)
Pine needles burning	0.86 ± 0.09	
Sesame stems burning	0.86 ± 0.09	
Rice straw burning	1.23 ± 0.33	(Fan et al., 2016)
Corn straw burning	1.56 ± 0.34	
Rice straw burning	0.79 ± 0.22	
Coal combustion	0.42 ± 0.03	
Source types	MSOC (365 nm)	Reference
Biodiesel/diesel	0.08–5.73	(Kuang et al., 2020)
Chemicals/diesel	ND–0.23	
Gasoline vehicle emission	0.62 ± 0.76	(Xie et al., 2017)
Biomass burning	1.27 ± 0.76	
Biomass burning	1.6 ± 0.55	(Tang et al., 2020)
Anthracite combustion	0.88 ± 0.74	
Bituminous coal combustion	3.2 ± 1.1	
Vehicle emission	0.26 ± 0.09	
Source types	DRI 2015 (405 nm)	Reference
Vehicle emission (tunnel)	1.0 ± 0.8	This study

previously measured by chassis dynamometer tests or at road sites (Schwarz et al., 2008; Cheng et al., 2011; Yan et al., 2019). It is unknown whether EC from on-road vehicles shows different MAE from that based on chassis dynamometer tests.

A previous study indicated that light-absorbing organic aerosols produced by low-temperature incomplete combustion (e.g., biomass combustion) had a stronger spectral dependence than those produced by high-temperature combustion processes (e.g., vehicles) (Kirchstetter et al., 2004). Therefore, much more attention has been paid to BrC from biomass burning than from vehicular emissions. However, in this study, the fleet average MAE_{405nm} of OC based on tunnel tests was 1.0 ± 0.8 $m^2\ g^{-1}$ C, which is higher than MAE_{365nm} from previous studies for vehicle emissions (Table 3), and even near that from biomass burning. It is worth noting that for vehicle-emitted OC the $MAE_{405\ nm}$ should be lower than $MAE_{365\ nm}$ (Fig. 5), implying that if the $MAE_{365\ nm}$ could be measured, it would be even higher than the reported $MAE_{365\ nm}$ in previous studies. A possible reason for this is that in previous studies, the BrC light absorption was measured with WSOC and MSOC by a UV–Vis spectrophotometer, and the extraction efficiency of light-absorbing OC by water and methanol may have great uncertainty. Interestingly, Liu et al. (2013) also found that the MAE_{365nm} of water-soluble OC (WSOC) or methanol-soluble OC (MSOC) in ambient aerosols collected at roadside was higher than that collected at the urban and rural sites, indicating BrC from vehicle emissions could contribute substantially to BrC particularly in urban areas. A possible reason for this is that in previous studies, the BrC light absorption was measured with WSOC and MSOC by a UV–Vis spectrophotometer, and the extraction efficiency of light-absorbing OC by water and methanol may have great uncertainty. Xie et al. (2017) indicated that while the methanol extraction efficiency was >90% for OC from biomass combustion, the methanol extraction efficiency of OC from vehicle exhausts was only 75.9%; therefore, if the non-extracted OC, like hydrophobic compounds with conjugated structures, contributes to the light absorption, the extraction method would underestimate the MAE of OC from vehicle exhausts. Nevertheless, there is still a lack of research on the difference of MAE_{OC} measured by the extraction method and the multi-wavelength thermal/optical carbon analyzer. Till now, there are quite limited studies using the multi-wavelength thermal/optical carbon analyzer to measure MAE_{OC} for filter-based ambient aerosol samples (Li et al., 2018; Zhao et al., 2019b; Peng et al., 2020). It is worth noting that Ghaffarpasand et al. (2020) recently revealed an increase in the NO_2/NO_x ratio in exhausts from EURO-VI vehicles. There is concern whether this elevated NO_2/NO_x ratio would facilitate the formation of more light-absorbing nitro-containing compounds (such as nitrophenols and nitro-PAHs) that would result in higher MAE values for vehicle-emitted OC (Liu et al., 2008; Chen and Bond, 2010; Zhang et al., 2013).

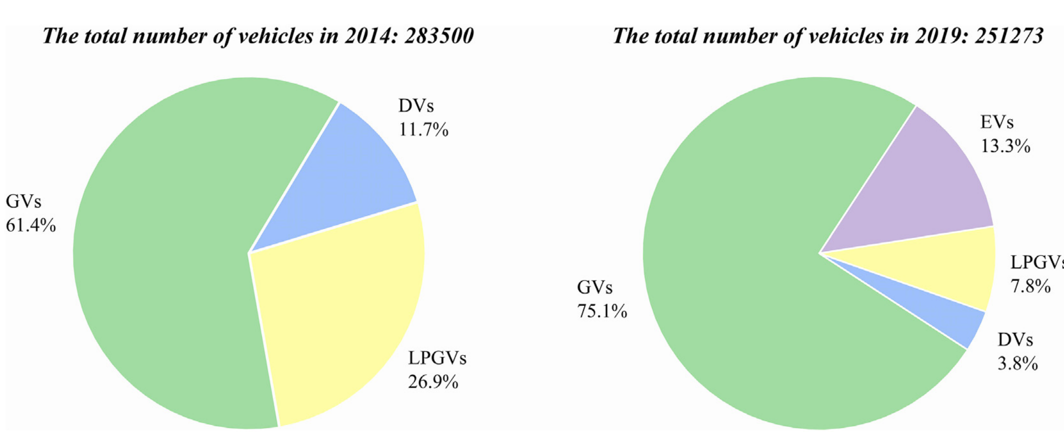

Fig. 7. The average proportions of different vehicles during the sampling period in 2014 and 2019.

4. Conclusions

In this study, carbonaceous aerosol emissions from on-road vehicles under real-world conditions were measured in a busy urban tunnel with traffic volumes of over 30,000 vehicles day^{-1}. We obtained a fleet-average TC-EF of 13.4 ± 8.3 mg veh^{-1} km^{-1}, in which the average OC-EF and EC-EF was 8.5 ± 6.6 and 4.9 ± 2.6 mg veh^{-1} km^{-1}, respectively. If EVs and LPGVs, which are free of carbonaceous aerosol emissions, were excluded in the vehicle fleets, the average for DVs and GVs in the fleets was 17.4 ± 11.3 mg veh^{-1} km^{-1}, in which the average OC-EF and EC-EF was 11.0 ± 8.8 and 6.3 ± 3.6 mg veh^{-1} km^{-1}, respectively. Compared to the EF measured in the same tunnel in 2014, the fleet-average EF from this study decreased by 59.0%, and the average OC-EF and EC-EF decreased by 56.0% and 63.5%, respectively. The ΔOC/ΔEC ratios ranged from 0.2 to 5.7 with an average of 1.8 ± 1.0.

Based on regression between fleet average EF and fleet compositions at different time intervals, the average TC-EF for DVs and GVs were derived. The average TC-EF for DVs (319.8 mg veh^{-1} km^{-1}) was more than 150 times that for GVs (2.1 mg veh^{-1} km^{-1}), and therefore DVs still dominate over GVs in on-road carbonaceous aerosol emissions, although DVs only shared 4% in the fleets.

By using a multi-wavelength thermal/optical carbon analyzer, the filter-based aerosol samples were further characterized for the light-absorbing properties of carbonaceous aerosols. The aerosol light absorption at 405, 455 and 635 nm were measured to be 45.5 ± 28.2, 41.4 ± 25.7, and 29.0 ± 18.0 Mm^{-1}, in which BrC contributed 19.1 ± 12.3%, 18.4 ± 11.7%, and 13.5 ± 9.1%, respectively.

The MAE_{EC} at 635 nm was calculated to be 5.2 m^2 g^{-1} C on average, lower than that previously tested by the chassis dynamometer. However, the average MAE_{OC} at 405 nm (1.0 ± 0.8 m^2 g^{-1} C) was higher than previously reported for vehicle emissions. Further studies, especially on a molecular level and morphological aspects, are needed to give an explanation for the lower MAE_{EC} and higher MAE_{OC} for on-road vehicular emissions.

Data availability

Data are available upon request from the corresponding author (wangxm@gig.ac.cn).

CRediT authorship contribution statement

Runqi Zhang: Formal analysis, Writing – original draft, Data curation. **Sheng Li:** Formal analysis, Data curation. **Xuewei Fu:** Formal analysis. **Chenglei Pei:** Investigation. **Zuzhao Huang:** Investigation. **Yujun Wang:** Investigation. **Yanning Chen:** Investigation. **Jianhong Yan:** Investigation. **Jun Wang:** Data curation. **Qingqing Yu:** Data curation. **Shilu Luo:** Investigation, Data curation. **Ming Zhu:** Investigation, Data curation. **Zhenfeng Wu:** Investigation, Data curation. **Hua Fang:** Investigation, Data curation. **Shaoxuan Xiao:** Investigation, Data curation. **Xiaoqing Huang:** Investigation, Data curation. **Jianqiang Zeng:** Investigation, Data curation. **Huina Zhang:** Investigation, Data curation. **Wei Song:** Data curation, Writing – review & editing. **Yanli Zhang:** Data curation, Writing – review & editing. **Xinhui Bi:** Data curation, Writing – review & editing. **Xinming Wang:** Data curation, Writing – review & editing.

Declaration of competing interest

The authors declare that they have no conflict of interest.

Acknowledgments

This study was funded by Natural Science Foundation of China (41961144029), the Chinese Academy of Sciences (QYZDJ-SSW-DQC032), Department of Science and Technology of Guangdong Province (2020B1212060053/2017BT01Z134/2019B121205006) and Hunan Provincial Key Research and Development Program (2018SK2039).

References

Akimoto, H., 2003. Global air quality and pollution. Science 302, 1716–1719.

Alander, T.J.A., Leskinen, A.P., Raunemaa, T.M., Rantanen, L., 2004. Characterization of diesel particles: effects of fuel reformulation, exhaust aftertreatment, and engine operation on particle carbon composition and volatility. Environ. Sci. Technol. 38, 2707–2714.

Allen, J.O., Mayo, P.R., Hughes, L.S., Salmon, L.G., Cass, G.R., 2001. Emissions of size-segregated aerosols from on-road vehicles in the Caldecott Tunnel. Environ. Sci. Technol. 35, 4189–4197.

Almeida, S.M., Pio, C.A., Freitas, M.C., Reis, M.A., Trancoso, M.A., 2005. Source apportionment of fine and coarse particulate matter in a sub-urban area at the Western European Coast. Atmos. Environ. 39, 3127–3138.

Artelt, S., Kock, H., Konig, H.P., Levsen, K., Rosner, G., 1999. Engine dynamometer experiments: platinum emissions from differently aged three-way catalytic converters. Atmos. Environ. 33, 3559–3567.

Bergstrom, R.W., Russell, P.B., Hignett, P., 2002. Wavelength dependence of the absorption of black carbon particles: predictions and results from the TARFOX experiment and implications for the aerosol single scattering albedo. J. Atmos. Sci. 59, 567–577.

Bishop, G.A., Stedman, D.H., 1996. Measuring the emissions of passing cars. Acc. Chem. Res. 29, 489–495.

Bond, T.C., Bergstrom, R.W., 2006. Light absorption by carbonaceous particles: an investigative review. Aerosol Sci. Technol. 40, 27–67.

Bond, T.C., Streets, D.G., Yarber, K.F., Nelson, S.M., Woo, J.H., Klimont, Z., 2004. A technology-based global inventory of black and organic carbon emissions from combustion. J. Geophys. Res.-Atmos. 109, D14203.

Bond, T.C., Bhardwaj, E., Dong, R., Jogani, R., Jung, S., Roden, C., Streets, D.G., Trautmann, N.M., 2007. Historical emissions of black and organic carbon aerosol from energy-related combustion, 1850–2000. Glob. Biogeochem. Cycles 21, GB2018.

Bond, T.C., Doherty, S.J., Fahey, D.W., Forster, P.M., Berntsen, T., DeAngelo, B.J., Flanner, M.G., Ghan, S., Kaercher, B., Koch, D., Kinne, S., Kondo, Y., Quinn, P.K., Sarofim, M.C., Schultz, M.G., Schulz, M., Venkataraman, C., Zhang, H., Zhang, S., Bellouin, N., Guttikunda, S.K., Hopke, P.K., Jacobson, M.Z., Kaiser, J.W., Klimont, Z., Lohmann, U., Schwarz, J.P., Shindell, D., Storelvmo, T., Warren, S.G., Zender, C.S., 2013. Bounding the role of black carbon in the climate system: a scientific assessment. J. Geophys. Res.-Atmos. 118, 5380–5552.

Cao, J.J., Wang, Q.Y., Chow, J.C., Watson, J.G., Tie, X.X., Shen, Z.X., Wang, P., An, Z.S., 2012. Impacts of aerosol compositions on visibility impairment in Xi'an, China. Atmos. Environ. 59, 559–566.

Che, H., Zhang, X., Li, Y., Zhou, Z., Qu, J.J., 2007. Horizontal visibility trends in China 1981–2005. Geophys. Res. Lett. 34, L24706.

Chen, L.W.A., Chow, J.C., Wang, X.L., Robles, J.A., Sumlin, B.J., Lowenthal, D.H., Zimmermann, R., Watson, J.G., 2015. Multi-wavelength optical measurement to enhance thermal/optical analysis for carbonaceous aerosol. Atmos. Measure. Techn. 8, 451–461.

Chen, Y., Bond, T.C., 2010. Light absorption by organic carbon from wood combustion. Atmos. Chem. Phys. 10, 1773–1787.

Cheng, Y., He, K.B., Zheng, M., Duan, F.K., Du, Z.Y., Ma, Y.L., Tan, J.H., Yang, F.M., Liu, J.M., Zhang, X.L., Weber, R.J., Bergin, M.H., Russell, A.G., 2011. Mass absorption efficiency of elemental carbon and water-soluble organic carbon in Beijing, China. Atmos. Chem. Phys. 11, 11497–11510.

Chiang, H.L., Huang, Y.S., 2009. Particulate matter emissions from on-road vehicles in a freeway tunnel study. Atmos. Environ. 43, 4014–4022.

Chirico, R., Prevot, A.S.H., DeCarlo, P.F., Heringa, M.F., Richter, R., Weingartner, E., Baltensperger, U., 2011. Aerosol and trace gas vehicle emission factors measured in a tunnel using an Aerosol Mass Spectrometer and other on-line instrumentation. Atmos. Environ. 45, 2182–2192.

Chow, J.C., Watson, J.G., 2002. $PM_{2.5}$ carbonate concentrations at regionally representative Interagency Monitoring of Protected Visual Environment sites. J. Geophys. Res.-Atmos. 107 (D21), 8344.

Clarke, A., McNaughton, C., Kapustin, V., Shinozuka, Y., Howell, S., Dibb, J., Zhou, J., Anderson, B., Brekhovskikh, V., Turner, H., Pinkerton, M., 2007. Biomass burning and pollution aerosol over North America: organic components and their influence on spectral optical properties and humidification response. J. Geophys. Res.-Atmos. 112, D12S18.

Cofala, J., Amann, M., Klimont, Z., Kupiainen, K., Hoeglund-Isaksson, L., 2007. Scenarios of global anthropogenic emissions of air pollutants and methane until 2030. Atmos. Environ. 41, 8486–8499.

Contini, D., Vecchi, R., Viana, M., 2018. Carbonaceous aerosols in the atmosphere. Atmosphere 9, 181.

Cui, M., Chen, Y.J., Tian, C.G., Zhang, F., Yan, C.Q., Zheng, M., 2016. Chemical composition of $PM_{2.5}$ from two tunnels with different vehicular fleet characteristics. Sci. Total Environ. 550, 123–132.

Dai, S., Bi, X., Chan, L.Y., He, J., Wang, B., Wang, X., Peng, P., Sheng, G., Fu, J., 2015. Chemical and stable carbon isotopic composition of $PM_{2.5}$ from on-road vehicle emissions in the PRD region and implications for vehicle emission control policy. Atmos. Chem. Phys. 15, 3097–3108.

Drozd, G.T., McNeill, V.F., 2014. Organic matrix effects on the formation of light-absorbing compounds from alpha-dicarbonyls in aqueous salt solution. Environ. Sci. Proc. Imp. 16, 741–747.

El Haddad, I., Marchand, N., Dron, J., Temime-Roussel, B., Quivet, E., Wortham, H., Jaffrezo, J.L., Baduel, C., Voisin, D., Besombes, J.L., Gille, G., 2009. Comprehensive primary particulate organic characterization of vehicular exhaust emissions in France. Atmos. Environ. 43, 6190–6198.

Fan, X.J., Wei, S.Y., Zhu, M.B., Song, J.Z., Peng, P.A., 2016. Comprehensive characterization of humic-like substances in smoke PM2.5 emitted from the combustion of biomass materials and fossil fuels. Atmos. Chem. Phys. 16, 13321–13340.

Favez, O., Alfaro, S.C., Sciare, J., Cachier, H., Abdelwahab, M.M., 2009. Ambient measurements of light-absorption by agricultural waste burning organic aerosols. J. Aerosol Sci. 40, 613–620.

Feng, Y., Ramanathan, V., Kotamarthi, V.R., 2013. Brown carbon: a significant atmospheric absorber of solar radiation? Atmos. Chem. Phys. 13, 8607–8621.

Gaga, E.O., Ari, A., Akyol, N., Uzmez, O.O., Kara, M., Chow, J.C., Watson, J.G., Ozel, E., Dogeroglu, T., Odabasi, M., 2018. Determination of real-world emission factors of trace metals, EC, OC, BTEX, and semivolatile organic compounds (PAHs, PCBs and PCNs) in a rural tunnel in Bilecik, Turkey. Sci. Total Environ. 643, 1285–1296.

Ghaffarpasand, O., Beddows, D.C.S., Ropkins, K., Pope, F.D., 2020. Real-world assessment of vehicle air pollutant emissions subset by vehicle type, fuel and EURO class: new findings from the recent UK EDAR field campaigns, and implications for emissions restricted zones. Sci. Total Environ. 734, 139416.

Gillies, J.A., Gertler, A.W., Sagebiel, J.C., Dippel, W.A., 2001. On-road particulate matter ($PM_{2.5}$ and PM_{10}) emissions in the Sepulveda Tunnel, Los Angeles, California. Environ. Sci. Technol. 35, 1054–1063.

Handler, M., Puls, C., Zbiral, J., Marr, I., Puxbaum, H., Limbeck, A., 2008. Size and composition of particulate emissions from motor vehicles in the Kaisermühlen-Tunnel, Vienna. Atmos. Environ. 42, 2173–2186.

He, K.B., Huo, H., Zhang, Q., He, D.Q., An, F., Wang, M., Walsh, M.P., 2005. Oil consumption and CO_2 emissions in China's road transport: current status, future trends, and policy implications. Energy Policy 33, 1499–1507.

He, L.Y., Hu, M., Zhang, Y.H., Huang, X.F., Yao, T.T., 2008. Fine particle emissions from on-road vehicles in the Zhujiang Tunnel, China. Environ. Sci. Technol. 42, 4461–4466.

Hecobian, A., Zhang, X., Zheng, M., Frank, N., Edgerton, E.S., Weber, R.J., 2010. Water-soluble organic aerosol material and the light-absorption characteristics of aqueous extracts measured over the Southeastern United States. Atmos. Chem. Phys. 10, 5965–5977.

Jo, D.S., Park, R.J., Lee, S., Kim, S.W., Zhang, X., 2016. A global simulation of brown carbon: implications for photochemistry and direct radiative effect. Atmos. Chem. Phys. 16, 3413–3432.

Kirchstetter, T.W., Novakov, T., Hobbs, P.V., 2004. Evidence that the spectral dependence of light absorption by aerosols is affected by organic carbon. J. Geophys. Res.-Atmos. 109, D21208.

Kuang, Y., Guo, Y., Chai, J., Shang, J., Zhu, J., Stevanovic, S., Ristovski, Z., 2020. Comparison of light absorption and oxidative potential of biodiesel/diesel and chemicals/diesel blends soot particles. J. Environ. Sci. 87, 184–193.

Li, M.J., Fan, X., Zhu, M.J., Zou, C.L., Song, J.Z., Wei, S.Y., Jia, W.L., Peng, P.A., 2019. Abundance and light absorption properties of brown carbon emitted from residential coal combustion in China. Environ. Sci. Technol. 53, 595–603.

Li, S., Zhu, M., Yang, W.Q., Tang, M.J., Huang, X.L., Yu, Y.G., Fang, H., Yu, X., Yu, Q., Fu, X.X., Song, W., Zhang, Y.L., Bi, X.H., Wang, X.M., 2018. Filter-based measurement of light absorption by brown carbon in $PM_{2.5}$ in a megacity in South China. Sci. Total Environ. 633, 1360–1369.

Liu, C., Huang, X., Lan, Z., He, L., 2012. A tunnel test for $PM_{2.5}$ emission factors of motor vehicles in Shenzhen. Environ. Sci. Technol. 35, 150–153.

Liu, J., Bergin, M., Guo, H., King, L., Kotra, N., Edgerton, E., Weber, R.J., 2013. Size-resolved measurements of brown carbon in water and methanol extracts and estimates of their contribution to ambient fine-particle light absorption. Atmos. Chem. Phys. 13, 12389–12404.

Liu, Y., Shao, M., Lu, S., Chang, C.C., Wang, J.L., Fu, L., 2008. Source apportionment of ambient volatile organic compounds in the Pearl River Delta, China: part II. Atmos. Environ. 42, 6261–6274.

Lough, G.C., Schauer, J.J., Lonneman, W.A., Allen, M.K., 2005. Summer and winter nonmethane hydrocarbon emissions from on-road motor vehicles in the Midwestern United States. J. Air Waste Manage. Assoc. 55, 629–646.

Ma, C.J., Tohno, S., Kasahara, M., 2004. A case study of the single and size-resolved particles in roadway tunnel in Seoul, Korea. Atmos. Environ. 38, 6673–6677.

Maji, K.J., Arora, M., Dikshit, A.K., 2018. Premature mortality attributable to $PM_{2.5}$ exposure and future policy roadmap for 'airpocalypse' affected Asian megacities. Process Saf. Environ. Prot. 118, 371–383.

Mancilla, Y., Mendoza, A., 2012. A tunnel study to characterize $PM_{2.5}$ emissions from gasoline-powered vehicles in Monterrey, Mexico. Atmos. Environ. 59, 449–460.

Maykut, N.N., Lewtas, J., Kim, E., Larson, T.V., 2003. Source apportionment of $PM_{2.5}$ at an urban IMPROVE site in Seattle, Washington. Environ. Sci. Technol. 37, 5135–5142.

Mordukhovich, I., Wilker, E., Suh, H., Wright, R., Sparrow, D., Vokonas, P.S., Schwartz, J., 2009. Black carbon exposure, oxidative stress genes, and blood pressure in a repeated-measures study. Environ. Health Perspect. 117, 1767–1772.

Niu, X., Chuang, H.C., Wang, X., Ho, S.S.H., Li, L., Qu, L., Chow, J.C., Watson, J.G., Sun, J., Lee, S., Cao, J., Ho, K.F., 2020. Cytotoxicity of $PM_{2.5}$ vehicular emissions in the Shing Mun Tunnel, Hong Kong. Environ. Pollut. 263, 114386.

Park, S.S., Yu, J., 2016. Chemical and light absorption properties of humic-like substances from biomass burning emissions under controlled combustion experiments. Atmos. Environ. 136, 114–122.

Peng, C., Yang, F.M., Tian, M., Shi, G.M., Li, L., Huang, R.J., Yao, X.J., Luo, B., Zhai, C.Z., Chen, Y., 2020. Brown carbon aerosol in two megacities in the Sichuan Basin of southwestern China: light absorption properties and implications. Sci. Total Environ. 719, 137483.

Petzold, A., Ogren, J.A., Fiebig, M., Laj, P., Li, S.M., Baltensperger, U., Holzer-Popp, T., Kinne, S., Pappalardo, G., Sugimoto, N., Wehrli, C., Wiedensohler, A., Zhang, X.Y., 2013. Recommendations for reporting "black carbon" measurements. Atmos. Chem. Phys. 13, 8365–8379.

Pio, C., Cerqueira, M., Harrison, R.M., Nunes, T., Mirante, F., Alves, C., Oliveira, C., Sanchez de la Campa, A., Artíñano, B., Matos, M., 2011. OC/EC ratio observations in Europe: re-thinking the approach for apportionment between primary and secondary organic carbon. Atmos. Environ. 45, 6121–6132.

Ramanathan, V., Crutzen, P.J., Kiehl, J.T., Rosenfeld, D., 2001. Atmosphere — aerosols, climate, and the hydrological cycle. Science 294, 2119–2124.

Ramanathan, V., Ramana, M.V., Roberts, G., Kim, D., Corrigan, C., Chung, C., Winker, D., 2007. Warming trends in Asia amplified by brown cloud solar absorption. Nature 448, 575–578.

Ristovski, Z.D., Jayaratne, E.R., Morawska, L., Ayoko, G.A., Lim, M., 2005. Particle and carbon dioxide emissions from passenger vehicles operating on unleaded petrol and LPG fuel. Sci. Total Environ. 345, 93–98.

Robert, M.A., VanBergen, S., Kleeman, M.J., Jakober, C.A., 2007. Size and composition distributions of particulate matter emissions: part 1 — light-duty gasoline vehicles. J. Air Waste Manage. Assoc. 57, 1414–1428.

Schmale, J., Shindell, D., von Schneidemesser, E., Chabay, I., Lawrence, M., 2014. Clean up our skies. Nature 515, 335–337.

Schwarz, J.P., Gao, R.S., Spackman, J.R., Watts, L.A., Thomson, D.S., Fahey, D.W., Ryerson, T.B., Peischl, J., Holloway, J.S., Trainer, M., Frost, G.J., Baynard, T., Lack, D.A., de Gouw, J.A., Warneke, C., Del Negro, L.A., 2008. Measurement of the mixing state, mass, and optical size of individual black carbon particles in urban and biomass burning emissions. Geophys. Res. Lett. 35, L13810.

Shang, Y., Sun, Z.W., Cao, J.J., Wang, X.M., Zhong, L.J., Bi, X.H., Li, H., Liu, W.X., Zhu, T., Huang, W., 2013. Systematic review of Chinese studies of short-term exposure to air pollution and daily mortality. Environ. Int. 54, 100–111.

Shen, X.B., Yao, Z.L., Huo, H., He, K.B., Zhang, Y.Z., Liu, H., Ye, Y., 2014. $PM_{2.5}$ emissions from light-duty gasoline vehicles in Beijing, China. Sci. Total Environ. 487, 521–527.

Shindell, D., Kuylenstierna, J.C.I., Vignati, E., van Dingenen, R., Amann, M., Klimont, Z., Anenberg, S.C., Muller, N., Janssens-Maenhout, G., Raes, F., Schwartz, J., Faluvegi, G., Pozzoli, L., Kupiainen, K., Hoeglund-Isaksson, L., Emberson, L., Streets, D., Ramanathan, V., Hicks, K., Oanh, N.T.K., Milly, G., Williams, M., Demkine, V., Fowler, D., 2012. Simultaneously mitigating near-term climate change and improving human health and food security. Science 335, 183–189.

Stewart, G.J., Nelson, B.S., Acton, W.J.F., Vaughan, A.R., Farren, N.J., Hopkins, J.R., Ward, M.W., Swift, S.J., Arya, R., Mondal, A., Jangirh, R., Ahlawat, S., Yadav, L., Sharma, S.K., Yunus, S.S.M., Hewitt, C.N., Nemitz, E., Mullinger, N., Gadi, R., Sahu, L.K., Tripathi, N., Rickard, A.R., Lee, J.D., Mandal, T.K., Hamilton, J.F., 2021. Emissions of intermediate-volatility and semi-volatile organic compounds from domestic fuels used in Delhi, India. Atmos. Chem. Phys. 21, 2407–2426.

Sun, H., Biedermann, L., Bond, T.C., 2007. Color of brown carbon: a model for ultraviolet and visible light absorption by organic carbon aerosol. Geophys. Res. Lett. 34, L17813.

Tang, J., Li, J., Su, T., Han, Y., Mo, Y., Jiang, H., Cui, M., Jiang, B., Chen, Y., Tang, J., Song, J., Peng, P.A., Zhang, G., 2020. Molecular compositions and optical properties of dissolved brown carbon in biomass burning, coal combustion, and vehicle emission aerosols illuminated by excitation-emission matrix spectroscopy and Fourier transform ion cyclotron resonance mass spectrometry analysis. Atmos. Chem. Phys. 20, 2513–2532.

Tie, X.X., Wu, D., Brasseur, G., 2009. Lung cancer mortality and exposure to atmospheric aerosol particles in Guangzhou, China. Atmos. Environ. 43, 2375–2377.

Wang, J.F., Ding, Y., Yin, H., Tan, J.W., Yin, B.H., 2013. A study on the characteristics of PM number emission from LPG vehicle. Automot. Eng. 35, 645–648.

Wang, R., Tao, S., Wang, W., Liu, J., Shen, H., Shen, G., Wang, B., Liu, X., Li, W., Huang, Y., Zhang, Y., Lu, Y., Chen, H., Chen, Y., Wang, C., Zhu, D., Wang, X., Li, B., Liu, W., Ma, J., 2012. Black carbon emissions in China from 1949 to 2050. Environ. Sci. Technol. 46, 7595–7603.

Wang, Z.S., Xiao, Z.C., Wang, H.P., Deng, B.Q., Liu, X.J., Li, L.G., Li, T., 2004. Study of the timing on characteristics of particulate emissions for LPG and gasoline fuels. Trans. CSICE 22, 56–62.

Wu, D., Bi, X.Y., Deng, X.J., Li, F., Tan, H., Liao, G., Huang, J., 2007. Effect of atmospheric haze on the deterioration of visibility over the Pearl River Delta. Acta Meteorol. Sin. 21, 215–223.

Xie, M., Hays, M.D., Holder, A.L., 2017. Light-absorbing organic carbon from prescribed and laboratory biomass burning and gasoline vehicle emissions. Sci. Rep. 7, 7318.

Yan, C.Q., Zheng, M., Shen, G.F., Cheng, Y., Ma, S.X., Sun, J.Z., Cui, M., Zhang, F., Han, Y., Chen, Y.J., 2019. Characterization of carbon fractions in carbonaceous aerosols from typical fossil fuel combustion sources. Fuel 254, 115620.

Yang, H.H., Dhital, N.B., Wang, L.C., Hsieh, Y.S., Lee, K.T., Hsu, Y.T., Huang, S.C., 2019. Chemical characterization of fine particulate matter in gasoline and diesel vehicle exhaust. Aerosol Air Qual. Res. 19, 1439–1449.

Yang, M., Howell, S.G., Zhuang, J., Huebert, B.J., 2009. Attribution of aerosol light absorption to black carbon, brown carbon, and dust in China — interpretations of atmospheric measurements during EAST-AIRE. Atmos. Chem. Phys. 9, 2035–2050.

Yao, Z.L., Shen, X.B., Ye, Y., Cao, X.Y., Jiang, X., Zhang, Y.Z., He, K.B., 2015. On-road emission characteristics of VOCs from diesel trucks in Beijing, China. Atmos. Environ. 103, 87–93.

Yu, L.D., Wang, G.F., Zhang, R.J., Zhang, L.M., Song, Y., Wu, B.B., Li, X.F., An, K., Chu, J.H., 2013. Characterization and source apportionment of $PM_{2.5}$ in an urban environment in Beijing. Aerosol Air Qual. Res. 13, 574–583.

Yuan, J.F., Huang, X.F., Cao, L.M., Cui, J., Zhu, Q., Huang, C.N., Lan, Z.J., He, L.Y., 2016. Light absorption of brown carbon aerosol in the PRD region of China. Atmos. Chem. Phys. 16, 1433–1443.

Zhai, H.B., Li, L.G., Liu, Z.M., Deng, B.Q., 2007. Characteristics of particulate emissions at idle from a small LPG EFI SI engines. Trans. CSICE 25, 66–72.

Zhang, Y.L., Wang, X.M., Barletta, B., Simpson, I.J., Blake, D.R., Fu, X.X., Zhang, Z., He, Q.F., Liu, T.Y., Zhao, X.Y., Ding, X., 2013. Source attributions of hazardous aromatic hydrocarbons in urban, suburban and rural areas in the Pearl River Delta (PRD) region. J. Hazard. Mater. 250, 403–411.

Zhang, Y.L., Wang, X.M., Li, G.H., Yang, W.Q., Huang, Z.H., Zhang, Z., Huang, X.Y., Deng, W., Liu, T., Huang, Z.Z., Zhang, Z.Y., 2015. Emission factors of fine particles, carbonaceous aerosols and traces gases from road vehicles: recent tests in an urban tunnel in the Pearl River Delta, China. Atmos. Environ. 122, 876–884.

Zhang, Y.L., Yang, W.Q., Simpson, I., Huang, X.Y., Yu, J.Z., Huang, Z.H., Wang, Z.Y., Zhang, Z., Liu, D., Huang, Z.Z., Wang, Y.J., Pei, C.L., Shao, M., Blake, D.R., Zheng, J.Y., Huang, Z.J., Wang, X.M., 2018. Decadal changes in emissions of volatile organic compounds (VOCs) from on-road vehicles with intensified automobile pollution control: case study in a busy urban tunnel in south China. Environ. Pollut. 233, 806–819.

Zhao, X.Y., Wang, J., Zhu, S.N., Bian, S.S., Zhang, Y., Wang, X.H., Yin, B.H., Yang, W., Bai, Z.P., 2019a. Emission characteristics of exhaust PM and its carbonaceous components from China III to China IV diesel vehicles in Shenyang. Huanjing Kexue 40, 4330–4336.

Zhao, Y.B., Gao, P.P., Yang, W.D., Ni, H.G., 2018. Vehicle exhaust: an overstated cause of haze in China. Sci. Total Environ. 612, 490–491.

Zhao, Z.Z., Cao, J.J., Chow, J.C., Watson, J.G., Chen, A.L.W., Wang, X.L., Wang, Q.Y., Tian, J., Shen, Z.X., Zhu, C.S., Liu, S.X., Tao, J., Ye, Z.L., Zhang, T., Zhou, J.M., Tian, R.X., 2019b. Multi-wavelength light absorption of black and brown carbon at a high-altitude site on the southeastern margin of the Tibetan Plateau, China. Atmos. Environ. 212, 54–64.